

THESIS DECLARATION

© This item is protected by original copyright

ACKNOWLEDGEMENT

Alhamdulillah, foremost, I would like to express my gratitude to my supervisor, Assoc. Prof. Dr. Mohd Fareq Abd Malek for the useful comments, remarks and engagement through the learning process of this thesis. I could not have imagined having a better supervisor.

Apart from the efforts of me, the success of this research depends largely on the encouragement and guidelines of many others. I take this opportunity to express my gratitude to the people who have been instrumental in the successful completion of this research. I would like to show my greatest appreciation to my co-supervisor, Prof. Dr. Syed Idris Syed Hassan, for enlightening me the first glance of research besides their encouragement, insightful comment.

Most importantly, none of this would have been possible without the love and patience of my family. My words will fail to express my heartfelt thanks especially to my beloved wife, Nurul Husna Abd Wahab, who has supported me throughout entire process, both by keeping me harmonious and helping me putting pieces together. And also my little, brilliant son, Muhammad Ayyash Muinuddin for inspiring me to work harder. I will be grateful forever for your love. As for my parent, receive my deepest gratitude and love for their endless love and support through these years.

Last but not least, I would like to thank the Advanced Communication Engineering (ACE), especially Assoc. Prof. Ir. Dr. Mohd Faizal bin Jamlos for aiding measurement tools. I am grateful for their constant support and help.

TABLE OF CONTENTS

THESIS DECLARATION	i
ACKNOWLEDGEMENT	ii
TABLE OF CONTENTS	iii
LIST OF FIGURES	vii
LIST OF TABLES	xi
LIST OF ABBREVIATIONS	xii
LIST OF SYMBOLS	xiii
ABSTRAK	xiv
ABSTRACT	xv
CHAPTER 1 INTRODUCTION	
1.1 Background	1
1.2 Problem Statement	2
1.3 Objectives of the Research Work	4
1.4 Contribution of the Thesis	5
1.5 Thesis Outline	6
CHAPTER 2 LITERATURE REVIEW	
2.1 Introduction	8
2.2 Radiation from Mobile Phones	9
2.3 Specific Absorption Rate (SAR)	10
2.3.1 Factors That Affect SAR	12
2.3.2 Transmitting Power	13

2.4	Biological Effects of EMF	15
2.4.1	Thermal Effects	15
2.4.2	Non-thermal Effect	17
2.5	Cognitive Effects of Microwave Exposure	17
2.6	Assessment of the Various Types of Metal Objects	18
2.7	Metal Objects Inside and Outside the Human Body Exposed to EMF	23
2.8	Brief Description of an Osseointegrated Ear Implant Retained Prosthesis	28
2.9	Simulation and Human Model	30
2.10	Properties of human body tissues	32
2.11	Effects of Hand Operation	35
2.12	Summary	35
CHAPTER 3 RESEARCH METHODOLOGY		
3.1	Introduction	37
3.2	Dipole Antenna as a RF Source	38
3.3	Head Models	40
3.3.1	Simple Geometrical Phantom Heads	40
3.3.2	Phantom Head Model	42
3.3.3	Voxel Head Model	42
3.4	Metal Objects	44
3.4.1	A Metal Rod as Simple, Metal-frame Glasses	44
3.4.2	Model based on the Frame of the Actual Glasses	45
3.4.3	Ear Implant	49
3.5	Measurement Setups	52
3.6	Summary	54

CHAPTER 4 SAR EVALUATION USING HOMOGENEOUS HEAD MODELS

4.1	Introduction	55
4.2	Validation of the Estimated SAR	56
4.3	Comparative Study of a Simple Geometrical Phantom Head	57
4.4	Results for Straight Metal Pin as Semi-rimless Glasses	61
4.5	Preliminary Investigation of the Effect of the Metal Object on the COST244 Head Model	66
4.5.1	Conductivity of the Metal Object as a Variable	66
4.5.2	Different Dimensions of the Head	68
4.5.3	Curvature of the Metal Rod	69
4.5.4	Using Different Radii of the Rod	70
4.6	Parameters that Influenced the SAR when an Ear Prosthesis Was Used	71
4.7	Side-Head Radiation Source (Situation 1)	75
4.7.1	Exposure 5 mm from the Head with Implant (PEC Bar)	76
4.7.2	Exposure 13 mm from the Head with Implant and Glasses	82
4.8	Frontal Face Radiation sources (Situation 2)	88
4.9	Summary	95

CHAPTER 5 SAR EVALUATION USING REALISTIC HUMAN TISSUES

5.1	Introduction	97
5.2	Radiation Source at the Side of the Head	97
5.3	Radiation Source in Front of the Face	107
5.4	SAR Validation Result	110
5.5	Summary	113

CHAPTER 6 CONCLUSIONS

6.1	Introduction	114
6.2	Summary	114
6.3	Future Research	117

REFERENCES	119
-------------------	-----

APPENDIXES	119
-------------------	-----

PUBLICATIONS	135
---------------------	-----

© This item is protected by original copyright

LIST OF FIGURES

NO.		PAGE
2.1	Electromagnetic spectrum.	9
2.2	(a) Ideal implant sites relative to the ear anatomy; (b) metal implant bar; (c) ear implant prosthesis; (d) clips as seen from back.	30
2.3	Effect of frequency on the characteristics of human tissues: (a) dielectric constant; (b) loss tangent; (c) conductivity	34
3.1	Research methodology used to evaluate SAR.	38
3.2	Performance magnitude of dipole antennas S_{11} (dB): (a) 900 MHz; (b) 1800 MHz; (c) 2100 MHz.	39
3.3	Basic shapes used as simple, geometrical phantom heads: (a) cylinder; (b) elliptical cylinder; (c) brick; (d) sphere.	41
3.4	Dimensions of the nose.	41
3.5	Dispersive properties of the TSL.	42
3.6	Two different head models: (a) SAM phantom head; (b) HUGO human head model at a resolution of 1 mm.	43
3.7	Position of the dipole antenna and metal rod: (a) top view; (b) side view The positions are as follows: The horizon distance from the dipole to the tip of the nose, m , was 100 mm, and the vertical distances from the tip of the nose to dipole and to the metal rod, n , was 44 mm.	45
3.8	Front view of full rim metal glasses: (a) actual glasses; (b) glasses after being modeled in the simulation.	46
3.9	Dimensions of common metal part of glasses: The length of arm, $a = 100.46$ mm, and the length of the frame, $b = 150.60$ mm.	47
3.10	(a) SAM phantom; (b) HUGO head-worn, metal frame glasses.	48
3.11	Dimensions of the implant: $a = 9.0$ mm; $b = 7.6$ mm; $c = 12.0$ mm; $d = 8.4$ mm; $e = 6.0$ mm; $f = 3.0$ mm.	49
3.12	Position of the implant relative to the head.	50
3.13	SAM phantom head with implanted metal bar: (a) side view; (b) front view.	50

3.14	Hugo head with implanted metal bar: (a) side view; (b) cross-section view at the y-z plane; (c) cross-section view at the z-x plane.	52
3.15	Signal generator used to generate a sine wave excitation at the desired frequency.	53
3.16	Measurement setup.	53
3.17	Simplified diagram of measurement for recording the local SAR.	54
4.1	Maximum SAR _{1g} level at 900 MHz for simple, geometrical models of heads:(a) without a nose; (b) with a nose.	58
4.2	Maximum SAR _{1g} level at 1800 MHz for simple, geometrical head models: (a) without a nose; (b) with a nose.	59
4.3	Maximum SAR _{1g} level at 2100 MHz for simple, geometrical head models: (a) without a nose; (b) with a nose.	60
4.4	SAR _{1g} distribution in SAM phantom head at the dipole separation distance of 30 mm.	60
4.5	SAR _{1g} distribution of the brick head model at 30 mm separation distance between the dipole and the head: (a) without a nose; (b) with nose.	61
4.6	SAR _{1g} (W/kg) with increasing length of the metal rod and separation distance from the surface of SAM: (a) 900 MHz; (b) 1800 MHz; (c) 2100 MHz.	63
4.7	SAR _{1g} distribution in a cross-section of the SAM phantom head for 2100 MHz: (a) without a metal rod; (b) with a metal rod.	64
4.8	SAM's cross-section view of electric field of 2100 MHz for the SAM phantom head: (a) without the rod; (b) with the rod.	65
4.9	Effect of conductivity of the rod material on SAR using a 900-MHz vertical dipole.	67
4.10	Effect of the radius of the spherical COST244 head on SAR with and without a rod.	68
4.11	A cross-section view of the head model from the top: By varying the radius of bending of the metal rod relative to the center of the head, it was possible to observe the effect of the curvature of the rod on the maximum SAR; The dipole antenna was aligned parallel to the rod, and the distances between the head and the dipole and head and the rod were 100 and 5 mm, respectively.	69
4.12	Maximum values of SAR at different radii of curvature relative to the center of the head model for 900 MHz.	70

4.13	Effect of the radius of the PEC rod on the value of SAR using a 900-MHz dipole.	71
4.14	Dimensions of a cross-section of a simple block ear: The radius of PEC rod embedded inside the ear was 0.25 mm.	72
4.15	The maximum SAR _{1g} versus relative permittivity of the simple block ear: (a) excitation at 900 MHz; (b) excitation at 1800 MHz; (c) excitation at 2100 MHz.	74
4.16	Trend of relative permittivity that caused the maximum SAR in the head with metal implanted in the ear at each frequency of RF exposure.	75
4.17	Maximum values of SAR as a function of the dipole's rotation angle at 900 MHz: (a) SAR _{1g} ; (b) SAR _{10g} .	78
4.18	Maximum values of SAR as a function of dipole's rotation angle at 1800 MHz: (a) SAR _{1g} ; (b) SAR _{10g} .	79
4.19	Maximum values of SAR as a function of the dipole's rotation angle at 2100 MHz with and without the implant: (a) SAR _{1g} ; (b) SAR _{10g} .	80
4.20	Distribution of local SAR through the x-y axis at 900 MHz for the head: (a) with implant; (b) without implant.	81
4.21	Maximum SARs as a function of the dipole's rotation angle at 900 MHz: (a) SAR _{1g} ; (b) SAR _{10g} .	84
4.22	Maximum SARs as a function of the dipole's rotation angle at 1800 MHz: (a) SAR _{1g} ; (b) SAR _{10g} .	85
4.23	Maximum SARs as a function of the dipole's rotation angle at 2100 MHz: (a) SAR _{1g} ; (b) SAR _{10g} .	87
4.24	3D SAR distribution at 2100 MHz: (a) averaged over 1 g; (b) averaged over 10 g.	87
4.25	Comparison of the SAR distribution (W/kg) in the head with glasses exposed to 900 MHz: (a) with the glass in place; (b) without the glass in place. The dipole antenna in front of the face was parallel (0 degree) to the glasses.	89
4.26	Distributions of maximum SAR _{1g} (W/kg) with the dipole positioned at 90 degrees at 900 Mhz : (a) 3D; (b) 2D.	90
4.27	Comparison of maximum SAR _{1g} (W/kg) in the head at 1800 MHz and the dipole at 30 degrees: (a) with glasses; (b) without glasses.	90
4.28	Comparison of maximum SAR _{1g} (W/kg) in the head at 1800 MHz With the dipole at 90 degrees: (a) with glasses; (b) without glasses.	91

4.29	Comparison of maximum SAR _{1g} (W/kg) in the head at 2100 MHz and the dipole at 90 degrees: (a) with glasses; (b) without glasses.	91
4.30	Maximum SARs as a function of the dipole's rotation angle in front of the face at 900 MHz: (a) SAR _{1g} ; (b) SAR _{10g} .	92
4.31	Maximum SAR as a function of the dipole's rotation angle in front of the face at 1800 MHz: (a) SAR _{1g} ; (b) SAR _{10g} .	93
4.32	Maximum SAR as a function of the dipole's rotation angle in front of the face at 2100 MHz: (a) SAR _{1g} ; (b) SAR _{10g} .	94
5.1	Maximum SAR _{1g} for the head at 900 MHz: (a) without metal; (b) with an ear implant; (c) with the combination of glasses and an implant.	99
5.2	SAR distribution in the head at 1800 MHz with the dipole aligned at 10 degrees: (a) without implant; (b) with implant.	100
5.3	SAR _{1g} distribution inside head (cross-sectional view in y-z axis)	101
5.4	Cross-section of head in the x-y axis.	101
5.5	SAR _{1g} distribution at 1800 MHz as comparison the head: (a) without implant; (b) with implant; (c) using the dipole aligned at 140 degrees	104
5.6	Cross-sectioned head in the x-y axis	105
5.7	E-field at 1800 MHz: (a) with only the implant; (b) with the implant and glasses with rubber ear support structures	106
5.8	Coupling mechanism of E-field between the metal implant and the antenna	107
5.9	Only at 900 SAR at ear highest: (a) head only, (b) glasses added, (c) implant and glasses.	110
5.10	Comparison of measured and simulated values of the local SAR with and without a metal rod at 1800 MHz.	112

LIST OF TABLES

NO.		PAGE
2.1	Comparison of the Output Powers of GSM and UMTS.	13
2.2	Summary of metal objects' interactions with the human body when exposed to EMF.	21
3.1	Radiation characteristics of the dipoles	40
4.1	Relationships between the ranges of optimum length that caused the maximum SAR_{lg} to the SAM compared to the length of the dipole.	64
5.1	Summary of the maximum SAR for the radiation source in front of the face	110

© This item is protected by original copyright

LIST OF ABBREVIATIONS

CAD	Computer aided design
CT	Computerized x-ray tomography
dB	Decibels
EM	Electromagnetic
EMF	Electromagnetic fields
FCC	Federal Communications Commission
FDTD	Finite-difference time-domain
ICNIRP	International Commission Non-Ionizing Radiation Protection
MRI	Magnetic resonance imaging
PEC	Perfect electrical conductor
RF	Radio frequency
SAM	Standard anthropomorphic model
SAR	Specific absorption rate
TSL	Tissue Simulating Liquid

LIST OF SYMBOLS

B	Magnetic flux density (W/m ²)
c	Speed of light (m/s)
C	Specific heat capacity (J/Kg·K)
D	Electric flux density (D/m ²)
E	Electric field
Je	Electric current (A/m ²)
Jm	Magnetic current (V/m ²)
SAR	Specific absorption rate (W/Kg)
λ	Wavelength (m)
σ	Conductivity (S/m)
ϵ	Electric permittivity (F/m)
μ	Magnetic permeability (H/m)
ρ	Density (Kg/m ³)

Kadar Penyerapan Khusus di Kepala Manusia Disebabkan Oleh Cermin Mata Bingkai-besi dan Protesis Telinga

ABSTRAK

Kajian di dalam tesis ini melibatkan penyiasatan kadar penyerapan tertentu (SAR) dalam model kepala manusia didedahkan kepada medan elektromagnet. SARs (1-g dan 10-g) telah dibandingkan dalam beberapa model kepala manusia. Siasatan ini bertujuan mengkaji kesan penggunaan cermin mata bingkai logam dan implan telinga prostetik yang realistik dikekalkan disambung pada sisi kepala. Satu set antena dwi-kutub yang beroperasi pada frekuensi umum 900, 1800 dan 2100 MHz telah dipusingkan untuk mengkaji kesan frekuensi dan polarisasi. Dua situasi dipertimbangkan dalam tesis; radiasi di bahagian hadapan muka, dan bahagian sisi kepala. Kajian awal telah dijalankan dengan menggunakan model kepala yang ringkas dan objek logam untuk meminimalkan tempoh simulasi. Empat jenis kepala bergeometri ringkas digunakan; bata, silinder, sfera dan silinder yang berbentuk elip disimulasikan dengan hidung dan tanpa hidung yang berbentuk ringkas untuk menyiasat sebarang kesan. Pada masa yang sama, rod logam lurus pada awalnya digunakan untuk mewakili cermin mata bingkai logam. Parameter telah diperluaskan lagi terhadap keberaliran rod logam yang berbeza, dimensi sebuah model kepala, kelengkungan rod dan jejari rod. Dalam kes radiasi sebelah sisi, penyiasatan telinga prostesis telah dimulakan dengan melihat kesan sifat dielektrik telinga tiruan yang berbeza. Selain itu, penggunaan gabungan objek logam ini yang mempunyai bentuk realistik bagi kedua-dua cermin mata dan implan (telinga) telah dikaji lebih terperinci dengan menggunakan model kepala manusia homogen dan heterogen. Keputusan ujikaji ini mencadangkan bahagian lain implan tersebut beresonansi bergantung pada frekuensi dan polarisasi, dan selanjutnya, menunjukkan bahawa implan ini nyata adalah elemen penyerakan. Implan menumpukan, fokus dan memantulkan tenaga frekuensi radio. Tisu yang berhampiran kepala juga akan mempunyai kesan muatan dielektrik sekunder. Peningkatan relatif kepada SAR_{10g} kerana implan yang jauh lebih kecil. Taburan SAR menunjukkan bahawa peningkatan pada SAR kerana implan logam tersebut amat setempat. Ini menerangkan perubahan dalam SAR_{1g} dan perubahan yang jauh lebih kecil untuk 10g SAR. Walau bagaimanapun, cermin mata bingkai logam yang dipilih dalam penyiasatan ini telah menunjukkan kenaikan SARs tidak ketara pada semua orientasi dwi-kutub dan frekuensi yang dipilih. Secara keseluruhannya, dengan mengambil kira telinga prostesis, pendedahan kepada 900 MHz daripada sebarang peranti berdekatan dengan implan tersebut mungkin boleh mengakibatkan kemudaratan. Ia juga dicadangkan supaya pesakit yang mempunyai telinga prostetik ini tidak boleh didedahkan kepada sebarang bentuk alat perhubungan berhampiran-badan pada sebarang julat frekuensi, kerana terdapat bukti bahawa logam diimplan di dalam bahan-bahan tertentu mempunyai perilaku berlainan untuk logam yang sama yang belum ditanam dalam sebarang bahan.

Specific Absorption Rate in the Human Head due to Metal-frame Glasses and Ear Prosthesis

ABSTRACT

The research in this thesis involves the investigation of the specific absorption rate (SAR) in a human head model exposed to electromagnetic fields. The SARs (1-g and 10-g) were compared inside various models of the human head. Investigation is aimed at the study of the effect of the use of a realistic implant retained prosthetic ear attached to the side of the head and metal-frame glasses. A set of dipole antennas operating at a common frequency of 900, 1800 and 2100 MHz were rotated to investigate the effect of frequency and polarization. Two situations were considered in the thesis; radiation at the front of the face, and at the side of the head. Initial studies were conducted using a simplified model of the head and metal object to minimize the duration of the simulation. Four types of simple geometrical head were used; brick, cylindrical, spherical and elliptical cylinders were simulated with and without the simple shape of the nose to investigate its possible effects. At the same time, a straight metal rod was initially employed to represent the metal-frame glasses. The parameters were further expanded to the different conductivities of the metal rod, the dimensions of a model of the head, the curvature of the rod and the radii of the rod. In the side radiation case, the investigation of the ear prosthesis was initiated by looking at the effect of different dielectric properties of the artificial ear. Moreover, the combined use of these metal objects with realistic shapes of both glasses and implant (ear) were investigated in detail using homogeneous and heterogeneous models of a human head. The results suggest that different sections of the implant resonate depending on the frequency and polarization, and furthermore, demonstrate that this real implant is a complex scattering element. The implant focuses and reflects the incident radio frequency (RF) energy. The nearby tissue of the head will also have a secondary dielectric loading effect. The relative enhancement on the SAR_{10g} due to the implant was much smaller. The SAR distribution shows that the increase in the SAR due to the metallic implant is extremely local with regards to the implant. This explains the change in the SAR_{1g} and the much smaller changes to the 10g SAR. However, the metal-frame glasses selected in this investigation had given a negative significant increment of SARs at any orientation of the dipole and frequency chosen. Overall, with regard to the ear prosthesis, exposure to 900 MHz from any device adjacent to the implant may cause harm. It also is suggested that patients with ear prostheses should not be exposed to any near-body communication at any frequency range, because there is evidence that metal implanted inside certain materials has different behavior from the same metal that has not been implanted in any material.

CHAPTER 1

INTRODUCTION

1.1 Background

In 1865, Maxwell formulated a set of equations as a first introduction to electromagnetic (EM) theory. The possibility of transmitting EM signals through the air was discovered in the late 19th century, but only in the past two decades the wireless communications become available to the general public, most notably through mobile phones. Over that period of time, the mobile communications industry has become economically important, especially in Finland, and a significant amount of research has managed to enhance the quality of wireless systems.

Radio frequency (RF) engineering and modern microwave engineering are exciting and vigorous topics, due in large part to the interaction between the advances in modern electronic technology and the increasing in demand for voice, data, and video communication capacity. Due to this major improvement in communications, mobile communication devices operating in the RF range have flourished rapidly in the market. Most notably, the smartphone almost has become a basic need for everyone. However, over the past few years, the possible consequences of the use of mobile phones on human health has been investigated by several researchers, (e.g., McIntosh, Anderson, & McKenzie, 2005; Siriwitprecha, Rattanadecho, & Wessapan, 2013; Virtanen, Huttunen, Toropainen, & Lappalainen, 2005; Virtanen, Keshvari, & Lappalainen, 2007).

Mobile phones are placed in close proximity to the user's head, hence, a certain amount of EM energy is absorbed by the head rather than being directly radiated. In addition, as the technology continues to improve, mobile phones will be used for various purposes and, therefore, the users will be exposed to EM energy for longer periods every day (Rahmat-Samii & Stutzman, 1998; W. G. Whittow, Edwards, Panagamuwa, & Vardaxoglou, 2008), and this may compound any possible health effects.

1.2 Problem Statement

The health effects of using mobile phones have been studied extensively in the past. Consequently, mandatory safety limits for RF energy absorption by human tissue have been established throughout the world. In order to minimize the heating effect on tissue caused by the absorption of RF energy by the human body, all mobile communications equipment (MCE) must comply with the regulations that establish the maximum power output of mobile phones.

The specific absorption rate (SAR) is used to evaluate the rate of absorption of energy by human tissue, and spatially-averaged SAR limits have been promulgated worldwide. For example, in the U.S. and Europe, the limits are 1.6 W/kg over 1 g of tissue and 2 W/kg over 10 g of tissue, respectively (ICNIRP, 1998; IEEE, 2005). Although RF emissions from mobile MCE are carefully regulated, the possibility exists that the RF characteristics are altered somewhat when tissue is irradiated by RF energy, thereby increasing the SAR.

Concern about the possible health effects due to exposure to electromagnetic fields (EMF) has increased among health professionals and the general public since

these communication devices were developed (Bernardi, Cavagnaro, Pisa, & Piuze, 2000; Cooper, & Hombach, 1996). This concern has caused an increase in the research conducted on the rate at which electromagnetic radiation is absorbed by the human body (Bernardi et al., 2000; Cooper & Hombach, 1998; Dimbylow, 2011). The issue is complicated further by the presence of any metal objects that may affect the characteristics of the EM radiation.

Furthermore, with recent advances in technology, mobile phones have been incorporated in a number of applications that require the device to be held in front of the face while transmitting. This introduces a new scenario in which both the side of the user's head and the user's face are exposed to the radiation source, which may be coupled with metal objects. In the past, several objects have been shown to alter the level of RF energy absorbed, including medical implants (Virtanen et al., 2007), metal-frame glasses (Troulis, Evans, Scanlon, & Trombino, 2003; W.G. Whittow & Edwards, 2004), and metal jewelry (W. G. Whittow et al., 2008).

More than a decade ago, rapid prototyping (RP) techniques began to be used extensively in maxillofacial surgery. This technique concentrates on producing exact physical replicas of patients' skeletal anatomy, and surgeons and prosthetists use the replicas to help plan reconstructive surgery and prosthetic rehabilitation. Developments in this area are moving rapidly towards the use of complex technologies to design and produce implants that make custom-fitted prostheses a reality. The definitive treatment for traumatic loss of an ear and poor surgical reconstruction often are followed by an implant-retained auricular prosthesis. As a result, there is increasing concern on the part of such patients about the health and safety aspects of such prostheses given the increasing use of RF devices, such as mobile phones, in close proximity to metal implants. In their initial study, Cooper & Hombach, (1996) concluded that the amount

of RF absorption within a homogeneous head model was enhanced substantially in the presence of metal implants. For example, the method used to retain an auricular prosthesis requires the use of a metal bar and a metal clip.

Thus, given the widespread application of bar and clip mechanisms in the production of prostheses for ears, it was deemed imperative to evaluate the compatibility between metal implants and EMF from RF devices, but, to date, this has not been done.

Furthermore, the combination of metal-frame glasses and an ear prosthesis could possibly result in a significant increase in the SAR. Again, no research addressing this issue can be found in the literature. It is hypothesized that SARs might increase at certain angles of incidence and frequency when the resonant frequency matches the length of the metal objects and is parallel to the excitation sources. It is predicted that an embedded metal implant inside different ear's tissues permittivity will produce different effects.

1.3 Objectives of the Research Work

The main objectives are to analyze the worst-case effects of metal-frame glasses and prosthetic ear implants on the SAR of energy by a human head when a subject is using common RF sources. The sources considered were mobile phones operating at 900, 1800, and 2100 MHz. The specific objectives are as follows:

- To determine the parameters that influence the RF energy coupling effect of a conductive metal rod in the human head.
- To model a 3D, realistic, metal-frame pair of glasses and an ear prosthesis for simulation in order to investigate the effect on human tissue.
- To evaluate the effect of an RF energy source on the SAR of a human head in the presence of both an ear prosthesis and metal-frame glasses.

1.4 Contribution of the Thesis

Changes in the SAR caused by metal objects in the presence of an RF energy source have received limited attention in the literature. In this thesis, the SAR in a model of a head exposed to EMF was analyzed while there was a 3D, implant-retained prosthetic ear attached to the side of the head. In addition, 3D, metal-frame glasses were added to evaluate the worst case scenario, i.e., when the person using the mobile phone has both of these metal objects on her or his head.

Different models of the human head were considered in the study. A simple homogeneous, spherical model of the head was used to validate the simulation with published results. Secondly, the head of a homogeneous specific anthropomorphic mannequin (SAM) used to observe the amount of RF energy the head absorbed. Then, the results were compared with the more realistic voxel model of the human head. Also, a cubical model of the head was used to compare the measurement and simulation results.

This thesis includes the effect of a real ear prosthesis and metal-frame glasses. To date, there have been very few research publications concerning the effect of an ear implant, i.e., cochlear implant, on the SAR in the head. However, it has been proven

that the presence of metal objects enhances the SAR. Thus, this thesis makes a new, important contribution to the knowledge in the field of bio-electromagnetics.

1.5 Thesis Outline

The thesis consists of six chapters, and the following five chapters are organized as follows; Chapter 2 provides a critical review of the effect of a metal object on the SAR, basic SARs for simulation and measurement, and the factors that affect the SAR. In this chapter, the interactions between the antenna, the human head, and metal objects also are discussed.

Chapter 3 deals with the methods and tools that were used in this research to investigate RF interactions with biological bodies. Chapter 3 also provides the validation procedure used to ensure that the simulation setup was designed appropriately before the simulation was conducted.

In Chapter 4, the results of the simulations are analyzed using tissue simulating liquid (TSL). In this chapter, four simple geometrical model of heads phantom are discussed with emphasis on the effect of the simple head with and without a simple geometrical human nose. The other parameters are varied in this chapter to determine the parameters that have the greatest effect on the SAR. The effects of orienting the dipole antenna in different directions were evaluated.

Chapter 5 investigated in detailed base on the results obtained from TSL and further studied with the voxel model of the human head for using the same source from an earlier chapter. The maximum SAR was studied in this chapter using the basis of the maximum SAR obtained from Chapter 4. This chapter also shows the measurement

results that indicate the effects of the metal objects on the SAR inside the cube head phantom model that filled with tissue-equivalent liquid.

Chapter 6 provides the conclusions based on the results of the simulations and experimental tests. Also, some recommendations for future work are presented.

© This item is protected by original copyright

CHAPTER 2

LITERATURE REVIEW

2.1 Introduction

In RF communication, there are two types of EMF situation; one is near field and the other is far field. In free space, the far field is straight forward because the electric field and the magnetic field are perpendicular to each other. In the context of analyzing the far field effect, exposure from a regular base station and simulation using a plane wave are used. Unlike the near field, the far field is much complex. In analyzing the near field for a device, such as a mobile phone used in close proximity to tissues, it is difficult to predict the EM field and other characteristics, since certain parts of the mobile phone scatter and reflect the EMF. The rationale for the studies of the effect of far field exposure is the work-related, high-level exposure of personnel while conducting their assigned tasks. Conversely, studies of the effect of near field exposure have resulted from public concern about the health risk associated with the use of RF devices in close proximity to the body. At the same time, carrying a metal object theoretically may enhance the possibility of RF absorption in certain cases. This is due to the complex reaction that occurs when EMF comes in contact with the surface of the human body. The transmitted RF energy may be absorbed by the human tissue (body), and or it may be reflected. The amounts of energy that are absorbed and reflected vary with the dielectric properties, the frequency of exposure, the shape of the exposed tissue, the angle of incidence, and the electrical conductivity of the tissues (Johnson &

Guy, 1972; Rani & Raju, 2013). Moreover, this absorption in the lossy tissues attenuates as the RF energy is absorbed by the tissue. In this chapter, reviews from the most-cited prior publications related to this research are discussed to determine their relevance and significance.

2.2 Radiation from Mobile Phones

Mobile phones broadcast in the microwave region, which is non-ionizing radiation. RF waves belong to the category of non-ionizing radiation because they cannot break chemical bonds or extract electrons from atoms, causing matter ionizing. Ionizing radiation causes biological effects because it breaks chemical bonds and creates ions. Thus, ionizing radiation is far more dangerous than non-ionizing radiation because it can cause distortions of the genetic and cause cancer (Holton, 2009). Figure 2.1 shows the microwave region of the electromagnetic spectrum.

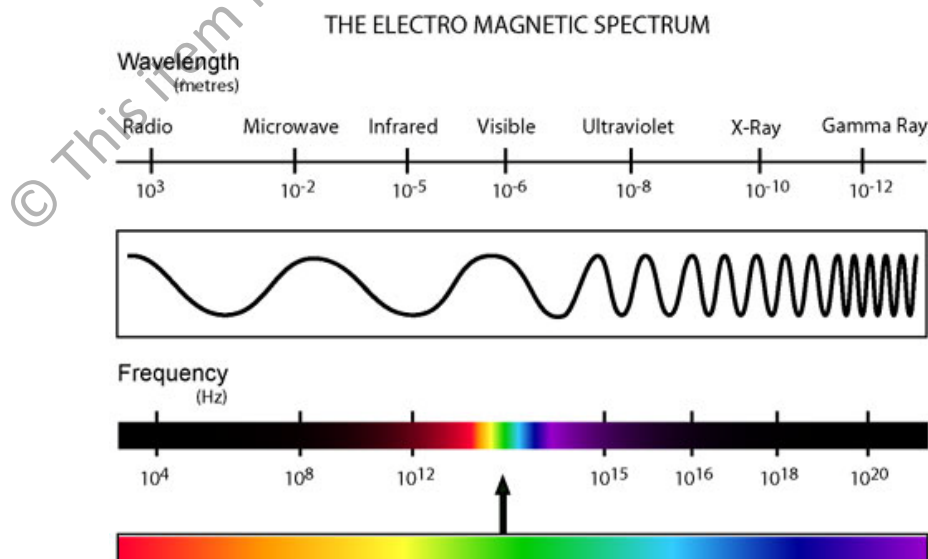


Figure 2.1: Electromagnetic spectrum (“electromagnetic spectrum,” n.d.).